ChemComm

COMMUNICATION

View Article Online
View Journal | View Issue

Cite this: *Chem. Commun.*, 2014, **50**, 14125

Received 7th July 2014,
Accepted 16th September 2014

DOI: 10.1039/c4cc05195e

www.rsc.org/chemcomm

Charge-transfer interactions for the fabrication of multifunctional viral nanoparticles†

Jun Hu,‡[ab] Peiyi Wang,‡[c] Xia Zhao,[a] Lin Lv,[b] Song Yang,[c] Baoan Song*[c] and Qian Wang*[b]

A facile strategy to fabricate multifunctional viral nanoparticles was described by introducing charge-transfer interactions between a pyrenyl motif with dinitrophenyl and pyridinium-contained guest molecules.

Significant progress has been made in the development of multifunctional nanoparticles for their wide biomedical applications in the past decades.[1] Specifically, viral nanoparticles (VNPs) derived from bacteria or plants have attracted considerable interest because of their multivalent programmable and monodispersed structures, as well as their low toxicity and good biocompatibility.[2] For better use of the inherent features of VNPs, a series of multifunctional VNPs has been fabricated by bio-orthogonal conjugation approaches, in which various targeting catalytic units, ligands, diagnostic probes and therapeutic cargoes have been modified on the surface or inside of the internal cavity of VNPs.[3]

However, these covalent-constructed methods are irreversible and normally require long reaction times and lengthy purification steps to introduce functional groups in the synthesis.[4] Consequently, supramolecular interactions are becoming more attractive because it is easy to realize the predictable change through attaching different stimuli-responsive groups on the basis of noncovalent synthesis, including hydrogen bonds, π-stacking, charge-transfer (CT) interactions, electrostatic interactions, and host–guest complexation.[5] In the supramolecular interactions family, CT interactions between electron-rich and electron-deficient species has been extensively applied to smart materials, self-assembly, drug and gene delivery due to its modularity, reversibility and stimuli-responsiveness.[6] For example, Huang and co-workers found that 2,4,6-trinitrotoluene (TNT) can be encapsulated by microtubes assembled from the pillar[5]arene amphiphile using CT interactions.[7a] Guchhait and co-workers successfully utilized the interactions of human serum albumin with a CT-probe (ethyl ester of *N*,*N*-dimethylamino naphthyl acrylic acid) to study the protein micro-environment.[7b] To date, reports on the application of CT-interactions modified VNPs are still rare,[8] though several works on protein modification using supramolecular interactions have been reported.[9]

Herein, we used the pyrene (**PYR**) moiety bearing a PEG chain to link the tobacco mosaic virus, **TMV(wt)**, consequently fabricating an electron-donor based on VNPs (Fig. 1a). **PYR** and its derivatives have been widely used as fluorescence probes in a large number of complex systems because of their high fluorescence quantum yields, long excited state lifetimes, and the ability to form excimers.[10] **TMV(wt)** is a model VNP having a rod-shape, 300 nm in length and 18 nm in diameter, consisting of 2130 identical subunit proteins arranged helically around a genomic single RNA strand.[11] On the other hand, dinitrophenyl and pyridinium-contained guest molecules (Fig. 1b) are chosen to be the electron-acceptors to form the CT complex.[12] The modified fluorescent **TMV(wt)-PYR** can form supra-amphiphiles with different electron-deficient molecules through CT interactions (Fig. 1c), in which a marked "switch off" of fluorescence from the **PYR** motif could be observed.

As shown in Fig. 1a, **PYR** was attached to the exterior surface of **TMV(wt)** by the sequential diazonium-coupling and Cu^{I}-catalyzed azide–alkyne cycloaddition (CuAAC) reaction (see ESI† for experimental details).[13] The formation of **TMV(wt)-PYR** was confirmed by UV-Vis and fluorescence spectra, as well as MALDI-TOF MS and SDS-PAGE analyses. As shown in Fig. 2a, two new peaks at 345 and 511 nm are observed. The peak at 345 nm is typical for the **PYR** group, while the peak at 511 nm could be attributed to the conjugative effect between the azobenzenyl and 1,2,3-triazole moieties, implying the successful attachment of the **PYR** moieties

[a] *State Key Lab of Polymer Physics and Chemistry, Changchun Institute of Applied Chemistry, Chinese Academy of Sciences, Changchun, 130022, China*
[b] *Department of Chemistry and Biochemistry, University of South Carolina, Columbia, SC 29208, USA. E-mail: wang263@mailbox.sc.edu*
[c] *State Key Lab Breeding Base of Green Pesticide & Agricultural Bioengineering Centre for R&D of Fine Chemicals, Guizhou University, Guiyang, 550025, China. E-mail: songbaoan22@yahoo.com*

† Electronic supplementary information (ESI) available: The details of instruments, reagents, and sample preparations; synthetic details, MS, and NMR spectra of **PYR-Azide**, **TMV(wt)-Alkyne**, **TMV(wt)-PYR**, **DNB**, **DDNB**, **DNB-Polyhema**, **MV**, **TV**, and **2-AP**; data of SDS-PAGE, SEC, DLS, TEM, and Job's plot. See DOI: 10.1039/c4cc05195e

‡ These two authors contribute equally to this work.

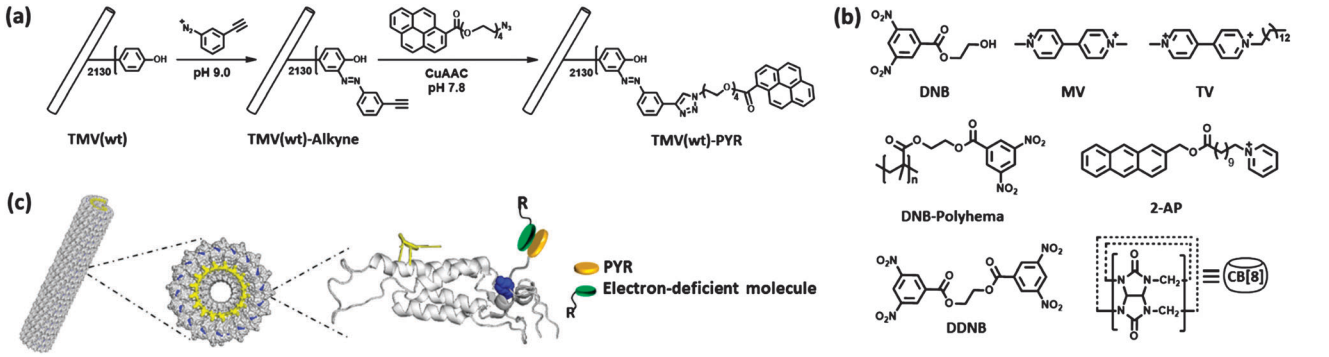

Fig. 1 (a) Preparation of **TMV(wt)-PYR** using diazonium-coupling and 'CuAAC' reactions. (b) Structures of electron-deficient guest molecules and **CB[8]**. (c) Schematic demonstration of the formation of multifunctional **TMV(wt)** *via* CT interactions between **PYR** and electron-deficient molecules.

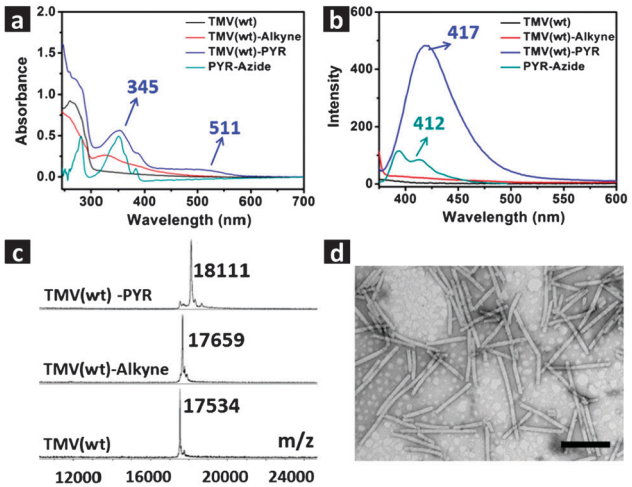

Fig. 2 (a) UV-Vis and (b) fluorescence spectra of **TMV(wt)**, **TMV(wt)-Alkyne**, **TMV(wt)-PYR**, and **PYR-Azide**. Excitation wavelength is 345 nm. (c) MALDI-TOF MS of the subunit proteins of **TMV(wt)**, **TMV(wt)**, and **TMV(wt)-PYR** the calculated MS for **TMV(wt)**, **TMV(wt)-Alkyne**, and **TMV(wt)-PYR** are 17 534, 17 662, and 18 109, respectively; the 452 *m/z* difference between **TMV(wt)-PYR** and **TMV(wt)-Alkyne** is consistent with the theoretical molar mass (447 *m/z*) of newly added **PYR-Azide** within the permitted error. (d) TEM image of uranyl acetate-stained **TMV(wt)-PYR**. Scale bar is 300 nm.

to the exterior surface of **TMV(wt)** by the 'CuAAC' reaction. This can be further verified by fluorescence spectra, in which **TMV(wt)-PYR** shows a strong fluorescence signal at 417 nm as compared to **TMV(wt)** and **TMV(wt)-Alkyne** (Fig. 2b). It should be noted that the slight wavelength shift between **TMV(wt)-PYR** and the small molecular **PYR-Azide** could be attributed to the intermolecular interactions of the **PYR** groups on the virus.[14] The MALDI-TOF MS result afforded the direct evidence for this complete conjugation reaction. As shown in Fig. 2c, the peak of the alkyne-modified **TMV(wt)** at *m/z* 17 659 disappears completely, while a new peak at *m/z* 18 111 is observed, indicating the full conversion of **TMV(wt)-Alkyne** to **TMV(wt)-PYR** upon conjugation. It is consistent with the results from the SDS-PAGE analysis (Fig. S1, ESI†). In addition, the integrity of the **TMV(wt)** nanoparticles upon conjugation was confirmed by size exclusion chromatography (SEC, Fig. S2, ESI†), transmission electron microscopy (TEM, Fig. 2d) and dynamic light scattering (DLS, Fig. S3, ESI†).

To test the CT interactions between **PYR** and electron-deficient molecules, six guest molecules, **DNB**, **DDNB**, **DNB-Polyhema**, **MV**, **TV**, and **2-AP** (Fig. 1b), were synthesized (see ESI† for experimental details). As a general protocol, **TMV(wt)-PYR** was incubated with electron-deficient molecules at different concentrations for 10 min at r.t. prior to fluorescence measurement. As shown in Fig. 3a, the fluorescence intensity of **TMV(wt)-PYR** is quenched dramatically upon the addition of **DNB**, revealing the CT interactions between **TMV(wt)-PYR** and **DNB**. The Job's plot shows a 1 : 1 complex formation for **TMV(wt)-PYR/DNB** (Fig. S4, ESI†),[15] which indicates that each **TMV(wt)-PYR** subunit associates with one **DNB** molecule. Other DNB-contained small molecules (**DDNB**) and polymers (**DNB-Polyhema**) were also tested using the aforementioned method. As shown in Fig. 3b and c, **DDNB** and **DNB-Polyhema** can quench the fluorescence of **PYR** with the binding modes as 1 : 2 and 1 : 1, respectively (Fig. S5 and S6, ESI†). Furthermore, there is no change in the integrity of **TMV(wt)-PYR** upon complexation, as observed with TEM (Fig. S7, ESI†). It is apparent that the DNB-contained electron-deficient molecules can form CT-complexes with the **TMV(wt)-PYR** nanoparticles. However, all the attempts to measure binding constants using isothermal titration calorimetry (ITC) failed, likely due to the existence of DMSO (as the co-solvent to dissolve the small molecules).

In contrast, when **MV** was used to form the CT-complex under the same condition as the DNB-derivatives, no obvious reduction in the emission could be observed (Fig. 3d). It was probably due to the electronic attractions between the positive charge of **MV** and the negative charge on **TMV(wt)**,[11] consequently leading to the absence of electron-deficient components for the formation of the CT-complex. To prohibit such binding, cucurbit-[8]uril (**CB[8]**) was used as a "molecular handcuff" to bring the **MV** and **PYR** moieties together.[16] It is known that **CB[8]** is a macrocyclic molecule that can form inclusive complexes with a high selectivity and binding affinity in aqueous media.[17] In addition, it was found that the size of **PYR** allowed the 1 : 1 complexation with **CB[8]**, and **CB[8]** is large enough to encapsulate two molecules at the same time. Therefore, we utilized **PYR** and **MV** as the guest for **CB[8]** to study their CT interactions in **CB[8]**. The emission spectra (Fig. 3e) indicate the formation of a supramolecular amphiphile because a significant fluorescence quenching effect could be observed from the CT interactions between **PYR** and **MV** inside the **CB[8]** cavity.

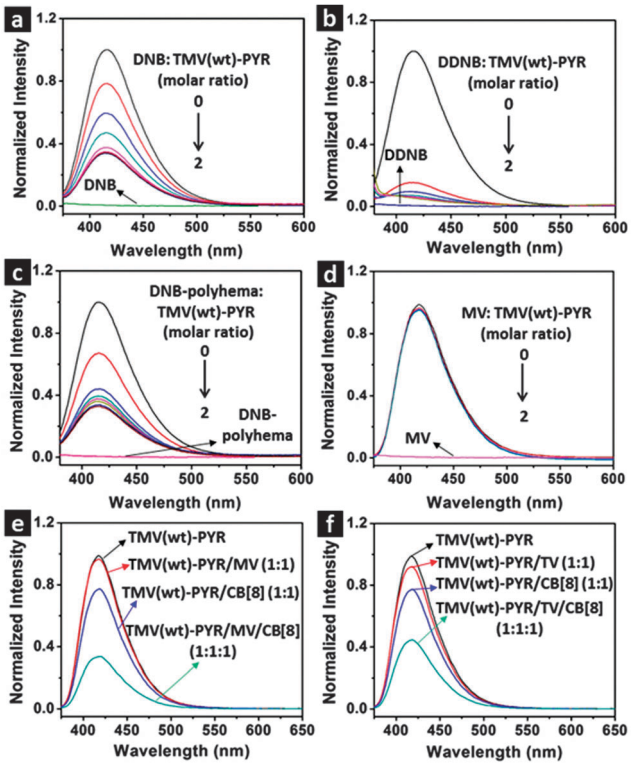

Fig. 3 Fluorescence spectra of **TMV(wt)-PYR** (0.38 mg mL^{-1} in K-phosphate buffer, pH 7.8) with (a) **DNB**, (b) **DDNB**, (c) **DNB-Polyhema**, and (d) **MV** with various molar ratios. Fluorescence spectra of (e) **TMV(wt)-PYR/MV** and (f) **TMV(wt)-PYR/TV** with the addition of **CB[8]**. Excitation wavelength is 345 nm.

Even in the absence of **MV**, a slight reduction in the fluorescence intensity was still detected due to the host–guest binding.[18] Moreover, the MV-derivative **TV** (Fig. 1b) with a long alkyl chain was also used to study the CT interactions with **TMV(wt)-PYR**. As shown in Fig. 3f, an emission quenching could be observed similar to the results from **MV**, which suggests that the MV-derivatives give a similar binding behavior as **MV**. The TEM image shows that there is no change in virus integrity after the complexation (Fig. S7, ESI†). Apparently, **TMV(wt)-PYR** could form the CT-complexes either with the neutral DNB-derivatives or positively-charged pyridinium-derivatives.

We have previously shown that **TMV** could be implanted in three-dimensional porous hydrogels, and such implanted **TMV** hydrogels can enhance cell attachment and promote the osteogenic differentiation of cultured stem cells.[19] Moreover, it exhibited a substantial decrease in immunity, low toxicity, and were degradable in mice.[20] Meanwhile, it is known that **2-AP** (Fig. 1b) bearing the electron-deficient pyridinium on their surface can assemble into ultralong nanofibers in K-phosphate buffer.[21] Inspired by above-mentioned results, we investigated if a supramolecular gel can be formed, driven by the CT interactions between **TMV(wt)-PYR** and the electron-deficient pyridiniums from the nanofiber surface. The results showed that a transparent supramolecular hydrogel formed with a T_g of 37 °C after mixing **TMV(wt)-PYR** and **2-AP** in a K-phosphate buffer (the critical gel concentration of **TMV(wt)-PYR** and **2-AP** are 0.12 and 3.0 mg mL^{-1}, respectively, pH 7.8, Fig. S8, ESI†).[22] Whereas under the same conditions, only a partial fragile hydrogel formed for **TMV(wt)**. It indicates that the CT interactions between the **PYR** moieties and the pyridiniums promote gelation. The detailed mechanism is being studied.

We demonstrated a facile strategy to fabricate multifunctional viral nanoparticles using CT interactions between pyrene-contained **TMV(wt)** nanoparticles with dinitrophenyl and pyridinium-based guest molecules. It is expected that the reversibility and the stimuli-responsive features of such supramolecular interactions can lead to the development of novel functional biomaterials.

This work is financially supported by US NSF-CHEM 1307319 and China Scholarship Council (200001). BS and SY thank the financial support of International Science & Technology Cooperation Program of China (2010DFB60840), National Key Program for Basic Research (2010CB126105), and National Nature Science Foundation of China (21132003). QW and JH are thankful for the support of State Key Laboratory of Polymer Physics and Chemistry, CIAC, China.

Notes and references

1 (*a*) J. Nicolas, S. Mura, D. Brambilla, N. Mackiewicz and P. Couvreur, *Chem. Soc. Rev.*, 2013, **42**, 1147; (*b*) A. M. Nyström and K. L. Wooley, *Acc. Chem. Res.*, 2011, **44**, 969; (*c*) J. Zhuang, M. R. Gordon, J. Ventura, L. Li and S. Thayumanavan, *Chem. Soc. Rev.*, 2013, **42**, 7421.
2 (*a*) H. N. Barnhill, S. Claudel-Gillet, R. Ziessel, L. J. Charbonnière and Q. Wang, *J. Am. Chem. Soc.*, 2007, **129**, 7799; (*b*) Y. Ma, R. J. M. Nolte and J. J. L. M. Cornelissen, *Adv. Drug Delivery Rev.*, 2012, **64**, 811; (*c*) J. K. Pokorski, K. Breitenkamp, L. O. Liepold, S. Qazi and M. G. Finn, *J. Am. Chem. Soc.*, 2011, **133**, 9242.
3 (*a*) J. D. Fiedler, S. D. Brown, J. L. Lau and M. G. Finn, *Angew. Chem., Int. Ed.*, 2010, **49**, 9648; (*b*) L. A. Lee, H. G. Nguyen and Q. Wang, *Org. Biomol. Chem.*, 2011, **9**, 6189; (*c*) P. Singh, M. J. Gonzalez and M. Manchester, *Drug Dev. Res.*, 2006, **67**, 23.
4 (*a*) A. C. Obermeyer, J. B. Jarman, C. Netirojjanakul, K. E. Muslemany and M. B. Francis, *Angew. Chem., Int. Ed.*, 2014, **53**, 1057; (*b*) R. Wang, D. M. Lockney, M. B. Goshe and S. Franzen, *Bioconjugate Chem.*, 2011, **22**, 1970; (*c*) C. R. Behrens, J. M. Hooker, A. C. Obermeyer, D. W. Romanini, E. M. Katz and M. B. Francis, *J. Am. Chem. Soc.*, 2011, **133**, 16398.
5 (*a*) A. Ajayaghosh and V. K. Praveen, *Acc. Chem. Res.*, 2007, **40**, 644; (*b*) A. Das and S. Ghosh, *Angew. Chem., Int. Ed.*, 2014, **53**, 1092; (*c*) C. Wang, Y. Guo, Y. Wang, H. Xu, R. Wang and X. Zhang, *Angew. Chem., Int. Ed.*, 2009, **48**, 8962.
6 (*a*) A. Das and S. Ghosh, *Angew. Chem., Int. Ed.*, 2014, **53**, 2038; (*b*) Y. S. Park, S. Y. Um and K. B. Yoon, *J. Am. Chem. Soc.*, 1999, **121**, 3193.
7 (*a*) Y. Yao, M. Xue, J. Chen, M. Zhang and F. Huang, *J. Am. Chem. Soc.*, 2012, **134**, 15712; (*b*) R. B. Singh, S. Mahanta, A. Bagchia and N. Guchhait, *Photochem. Photobiol. Sci.*, 2009, **8**, 101.
8 L. Chen, X. Zhao, Y. Lin, Y. Huang and Q. Wang, *Chem. Commun.*, 2013, **49**, 9678.
9 (*a*) Y. Yeh, S. Rana, R. Mout, B. Yan, F. S. Alfonsoa and V. M. Rotello, *Chem. Commun.*, 2014, **50**, 5565; (*b*) K. D. Daze, T. Pinter, C. S. Beshara, A. Ibraheem, S. A. Minaker, M. C. F. Ma, R. J. M. Courtemanche, R. E. Campbell and F. Hof, *Chem. Sci.*, 2012, **3**, 2695; (*c*) H. D. Nguyen, D. T. Dang, J. L. L. van Dongen and L. Brunsveld, *Angew. Chem., Int. Ed.*, 2010, **49**, 895.
10 (*a*) S. Dong, L. Gao, J. Chen, G. Yu, B. Zheng and F. Huang, *Polym. Chem.*, 2013, **4**, 882; (*b*) F. Li, Q. Song, L. L. Yang, G. L. Wu and X. Zhang, *Chem. Commun.*, 2013, **49**, 1808.
11 Z. Liu, J. Qiao, Z. Niu and Q. Wang, *Chem. Soc. Rev.*, 2012, **41**, 6178.
12 (*a*) K. V. Rao, K. Jayaramulu, T. K. Maji and S. J. George, *Angew. Chem., Int. Ed.*, 2010, **122**, 4314; (*b*) C. Wang, S. Yin, S. Chen, H. Xu, Z. Wang and X. Zhang, *Angew. Chem., Int. Ed.*, 2008, **47**, 9049.
13 T. L. Schlick, Z. B. Ding, E. W. Kovacs and M. B. Francis, *J. Am. Chem. Soc.*, 2005, **127**, 3718.

14 (*a*) W. Li, L. Wang, J. P. Zhang and H. Wang, *J. Mater. Chem.*, 2014, **2**, 1887; (*b*) G. X. Liu, Z. Y. Li, D. Wu, W. Xue, T. T. Li, S. H. Liu and J. Yie, *J. Org. Chem.*, 2014, **79**, 643.
15 (*a*) H. A. Benesi and J. H. Hildebrand, *J. Am. Chem. Soc.*, 1949, **71**, 2703; (*b*) H. M. Colquhoun, E. P. Goodings, J. M. Maud, J. F. Stoddart, J. B. Wolstenholme and D. J. Williams, *J. Chem. Soc., Perkin Trans. 2*, 1985, 607.
16 H. J. Kim, J. Heo, W. S. Jeon, E. Lee, J. Kim, S. Sakamoto, K. Yamaguchi and K. Kim, *Angew. Chem., Int. Ed.*, 2001, **40**, 1526.
17 (*a*) D. Jiao, F. Biedermann and O. A. Scherman, *Org. Lett.*, 2011, **13**, 3044; (*b*) D. Jiao, J. Geng, X. J. Loh, D. Das, T.-C. Lee and O. A. Scherman, *Angew. Chem., Int. Ed.*, 2012, **51**, 9633.
18 D. Jiao, F. Biedermann, F. Tian and O. A. Scherman, *J. Am. Chem. Soc.*, 2010, **132**, 15734.
19 (*a*) J. Luckanagul, L. A. Lee, Q. L. Nguyen, P. Sitasuwan, X. Yang, T. Shazly and Q. Wang, *Biomacromolecules*, 2012, **13**, 3949; (*b*) P. Sitasuwan, L. A. Lee, P. Bo, E. N. Davis, Y. Lin and Q. Wang, *Integr. Biol.*, 2012, **4**, 651.
20 J. Luckanagul, L. A. Lee, S. You, X. Yang and Q. Wang, *J. Biomed. Mater. Res., Part A*, 2014, DOI: 10.1002/jbm.a.35227.
21 J. Hu, P. Wang, Y. Lin, S. Yang, B. Song and Q. Wang, *Org. Biomol. Chem.*, 2014, **12**, 4820.
22 (*a*) H. Kar and S. Ghosh, *Chem. Commun.*, 2014, **50**, 1064; (*b*) H. Kar, M. R. Molla and S. Ghosh, *Chem. Commun.*, 2013, **49**, 4220.

